KINETICS OF NUCLEATION-CONTROLLED POLYMERIZATION

A Perturbation Treatment for Use with a Secondary Pathway

MARILYN F. BISHOP AND FRANK A. FERRONE
Department of Physics and Atmospheric Science, Drexel University, Philadelphia, Pennsylvania 19104

ABSTRACT We present a perturbation method for analyzing nucleation-controlled polymerization augmented by a secondary pathway for polymer growth. With this method, the solution to the kinetic equations assumes a simple analytic closed form that can easily be used in fitting data. So long as the formation of polymers by the secondary pathway depends linearly on the concentration of monomers polymerized, the form of the solutions is the same. This permits the analysis of augmented growth models with a minimum number of modeling assumptions, and thus makes it readily possible to distinguish between a variety of secondary processes (heterogeneous nucleation, lateral growth, and fragmentation). In addition, the parameters of the homogeneous process, such as the homogeneous nucleus size, can be determined independent of the nature of the secondary mechanism. We describe applications of this method to the polymerization of actin, collagen, and sickle hemoglobin. We present an extensive analysis of data on actin polymerization (Wegner, A., and P. Savko, 1982, *Biochemistry*, 21:1909–1913) to illustrate the use of the method. Although our conclusions generally agree with theirs, we find that lateral growth describes the secondary pathway better than the fragmentation model originally proposed. We also show how this method can be used to study the degree of polymerization, the parentage of polymers, and the behavior of polymers in cycling experiments.

INTRODUCTION

For a number of biological molecules (1–7), polymerization into larger structures involves a set of necessary but unfavorable steps in the reaction that bottleneck the formation of large aggregates. These steps are viewed as constituting formation of a critical nucleus. In any assembly process, the formation of intermolecular bonds competes with the greater translational and rotational entropy of monomers in solution. From a thermodynamic viewpoint, the nucleus represents a turning point in the balance between lost entropy and bond energy, i.e., an aggregate is postnuclear if, for a given concentration of monomers, the addition of a monomer adds to its stability, rather than increasing its instability. Kinetically this means that the rate of monomer addition to the aggregate exceeds the rate of monomer loss after the nucleus size is surpassed, but not before. Often such a nucleus is visualized as the result of some singular steric step, such as the closure of a ring, or a tube, or the completion of the first turn of a helix. However, it is clear that nucleation theories do not require such a special structure for the turning point in stability, and, in fact, the experimental evidence on assembling systems has not generally turned up such special structures.

Typically, the complete mathematical description of a polymerizing system requires a differential equation for the concentration of each aggregate, and even allowing only monomer addition or loss means that each equation will contain concentrations of aggregates of neighboring size. Moreover, the rate constants are not size independent until rather large polymers are reached. Thus, a complete treatment is a formidable problem. A simplifying strategem for nucleating systems is to assume that the subnuclear species are in equilibrium and thus calculate the concentration of nuclei as an equilibrium problem. As is done with transition state theory, this approach reduces a kinetic problem to an equilibrium one. Then monomer addition above nuclear size is assumed to proceed at rates appropriate to the rate constants for long polymers. Oosawa has presented such an approach for one-dimensional irreversible growth and has obtained simple closed form solutions to the kinetic equations (1, 8).

Despite many successes, there is ample evidence that this simple model does not fully describe the kinetics of such self-assembly systems as actin (9, 10), collagen (11, 12), or sickle cell hemoglobin (13, 14). The most notable discrepancy between theory and experiment is found in the time course of the reaction. In the three cases just mentioned, the concentration of polymerized monomers increases much more abruptly than the t^2 dependence that the Oosawa theory predicts. To describe this autocatalysis, the theory has been extended to include mechanisms by which polymers may form,

BIOPHYS. J. © Biophysical Society · 0006-3495/84/11/631/14 $1.00
Volume 46 November 1984 631–644

other than by straightforward homogeneous nucleation. For actin, fragmentation has been proposed as a secondary mechanism for polymer formation (9, 10). For sickle cell hemoglobin, heterogeneous nucleation of polymers onto the surface of other polymers acts as a secondary pathway (14). For collagen, it is clear that polymerization involves more than one pathway, although the nature of the initial steps in the process are in dispute (11, 12).

In practice, the comparison of such augmented nucleation mechanisms with experiments has been cumbersome because analytic solutions have not been known. Trial parameters must be used to produce kinetic curves that can then be compared with the data. Fitting is done by repeated iteration, which can be a slow and tedious process if several parameters are involved. Such procedures are ill-suited to the task of distinguishing between plausible mechanisms (e.g., secondary nucleation vs. fragmentation) because of the need to demonstrate that a given failure is not merely a poor choice of parameters. Conceptually, they are cumbersome as well because the sensitivity of the resulting solutions to input parameters is not readily apparent.

We find that these difficulties can be avoided by solving the same rate equations by a perturbation approach. In this method, we expand the concentrations of polymers and polymerized monomers about their initial values and retain only the lowest order terms in the rate equations. In lowest order, the equations become linear with simple analytic solutions. Of course this approach is valid only for studying the initial phase of the assembly reaction; however, this is not a severe limitation, because most of the kinetic information can be extracted from this portion of the data. In fact, for systems in which a dense network of polymers is formed (such as sickle cell hemoglobin), interpretation of the initial behavior in which the polymers remain dilute may also provide the most reliable data.

We find that the solution to the linearized equations has a form that is independent of the exact mechanism chosen to augment the primary nucleation pathway. Analysis of kinetic data in terms of this description yields parameters with a simple and direct relationship to fundamental kinetic constants. Moreover, a particular combination of parameters in this description is totally independent of the secondary process, allowing the primary nucleation step to be studied despite the strong possibility that the secondary process may have a dominant role in the kinetic behavior. Furthermore, the parameters in this description have simple, intuitive relationships to the shape of kinetic progress curves.

This paper is organized as follows. In the Formulation of the Problem section, we describe the basic augmented nucleation models and show how fragmentation, lateral growth, and secondary nucleation all produce formally similar equations. In the First-Order Solution section, we solve the general equations by use of perturbation theory. In the Accuracy of the Expansion section, we consider the accuracy of the theory used and the criteria that can be used to test for a given degree of accuracy. In the Actin section, we describe the application of this method to actin polymerization. We include an extensive analysis of published data here so that actin can serve as a model for use of the method. In addition, we compare the conclusions obtained here with the conclusions of others who numerically integrated the kinetic equations. In the Collagen section, we consider collagen polymerization as a possible example of nucleated polymerization with lateral growth and show that the slope of log-log plots of delay time vs. concentration may give an incorrect nucleus size. In the Further Applications section, we present three other general applications: the degree of polymerization, the parentage of polymers, and the analysis of depolymerization-repolymerization or cycling experiments. In the Conclusions, we summarize the usefulness of the method presented here. In the Appendix, we describe the modifications required to use this method for the analysis of polymerization in the presence of substantial solution nonideality (e.g., sickle hemoglobin).

FORMULATION OF THE PROBLEM

In this section, we formulate the differential equations that describe polymerization via two pathways. The primary pathway is homogeneous nucleation, which we describe by classical equilibrium nucleation theory. The principal assumption of this theory is that all polymerization processes are sufficiently slow to allow equilibrium to be established between nuclei and monomers. Since this theory is thoroughly described elsewhere (15, 16), we concentrate here on showing the various ways in which homogeneous nucleation can be augmented in the formation of polymers.

Our interest centers on two quantities: the concentration of polymerized monomers, denoted $\Delta(t)$, and the concentration of polymers, $c_p(t)$. We include in c_p any aggregate larger than a nucleus. Prenuclear aggregates are assumed to be in equilibrium with the monomer population. In addition, they are assumed to have concentrations much smaller than either the free-monomer concentration $c(t)$ or the concentration of polymerized monomers $\Delta(t)$. Therefore, if c_0 is the total monomer concentration, then $\Delta(t)$ is given by

$$\Delta(t) = c_0 - c(t). \tag{1}$$

$\Delta(t)$ changes through addition or loss of monomers at polymer ends. The rates of these processes, and thus the corresponding rate constants, are essentially independent of length for sufficiently long polymers. We assume this to be true for most of the polymers in the system, and we thus take association and dissociation to be described by simple rate constants, k_+ and k_-. Then the concentration of

incorporated monomers changes according to

$$\frac{d\Delta}{dt} = (k_+c - k_-)c_p. \quad (2)$$

It is often convenient to relate k_- to a solubility c_s by putting $k_- = k_+c_s$. Then the reaction naturally ceases when $c(t) = c_s$.

If we define a polymer as any species of size $i + 1$ or larger, then we can write the rate of homogeneously formed polymers as

$$\frac{dc_p}{dt} = k_+cc_i - k_-^*c_{i+1}. \quad (3)$$

The rate constant for monomer addition has again been taken as k_+. We shall, for simplicity, omit the k_-^* term.[1] In most cases this omission is experimentally indistinguishable from equating k_-^* to k_-, since k_+c is so much greater, especially in the initial phase of the reaction. Because the method we are developing here is limited to the initial phase of the reaction, this is a consistent approximation. Dropping the second term in Eq. 3, we can write the rate of polymer formation via the homogeneous pathway as

$$\frac{dc_p}{dt} = k_+cc_i = k_+K_ic^{i+1}. \quad (4)$$

In the last substitution, we explicitly invoke equilibrium nucleation theory by assuming that the nucleus of size i is in equilibrium with the monomer population, i.e., $c_i = K_ic^i$, where K_i is the rate constant for formation of a nucleus.

Fragmentation is one means of augmenting the formation of polymers. A simple description of fragmentation is to assume that polymers break at a rate proportional to their length. For a linear polymer, the length is simply proportional to $c_0 - c$, so that the full expression for polymer formation becomes

$$\frac{dc_p}{dt} = k_+K_ic^{i+1} + k_{fr}(c_0 - c). \quad (5)$$

The constant k_{fr} is the rate of polymer fragmentation. Wegner and Savko (10) have proposed that such a fragmentation mechanism occurs in actin polymerization. Our Eq. 5 is essentially their Eq. 7, except for the omission of monomer dissociation from nuclei. (See discussion above.)

Nucleation of additional polymers at the surfaces of existing polymers, called heterogeneous nucleation, is another means of augmenting polymer formation. The concentration of sites to which such heterogeneous nuclei attach and grow scales as the concentration of monomers already incorporated into polymers. Thus the concentration of polymers formed by this secondary mechanism scales as $(c_0 - c)$, as in the case of fragmentation. If we denote by ϕ the probability that a given polymer site can support heterogeneous nucleation, then the full expression for polymer formation becomes

$$\frac{dc_p}{dt} = k_+K_ic^{i+1} + k_+\phi\tilde{K}_jc^{j+1}(c_0 - c). \quad (6)$$

Here $\tilde{K}_j$ is the equilibrium constant for forming nuclei of size j and attaching them to surface sites, where again we have applied equilibrium nucleation theory. Ferrone et al. (14) have suggested that this mechanism describes the polymerization of sickle hemoglobin. Our Eq. 6 is essentially their Eq. 6a, except for the omission of activity coefficients. The treatment of nonideal solutions will be dealt with in the Appendix.

A special case of heterogeneous nucleation is lateral, non-nucleated growth. The distinction between lateral growth and heterogeneous nucleation is the same as that between isodesmic growth and homogeneous nucleation, i.e., for growth each step is favorable, and there is no nucleus to act as a limiter of the reaction rate. If ϕ is defined as above, and we define k_+' as the rate of association laterally, then this form of augmentation can be written as

$$\frac{dc_p}{dt} = k_+K_ic^{i+1} + \phi k_+'c(c_0 - c). \quad (7)$$

Such lateral association may apply to the kinetics of collagen polymerization (See the Collagen section).

Thus we find that a variety of augmented nucleation mechanisms have the general form

$$\frac{dc_p}{dt} = k_+K_ic^{i+1} + Q(c_0 - c) \quad (8)$$

where Q is given in Table I. In the First-Order Solution section we show how such equations may be solved by a perturbation approach, and we will see that the solution obtained does not depend upon the exact form of Q.

FIRST-ORDER SOLUTION

Because the kinetic equations described in the Formulation of the Problem section are not readily soluble in closed form, we will solve them by perturbation methods (17). This involves three steps. First, we expand all terms in the

TABLE I
SECONDARY PROCESSES

Type	Example	Q
Fragmentation	Actin	k_{fr}
Heterogeneous nucleation	Sickle hemoglobin	$k_+\phi\tilde{K}_jc^{j+1}$
Lateral growth	Collagen ?	$\phi k_+'c$

[1]Generally, k_-^* is not equal to k_- (in contrast to, e.g., reference 10). This follows from the definitions since k_- is the asymptotic limit of the dissociation rate for infinitely long polymers, whereas k_-^* is the first dissociation rate constant to decrease with aggregate size. In other words, at the step $i + 1$, the association rate exceeds the dissociation rate for the first time.

kinetic equations in power series in Δ and c_p. Second, we truncate the resulting equations, retaining up to first-order terms in Δ and c_p. Third, we solve these equations, obtaining a first-order approximation to the complete solution. If this approximate solution is not adequate, greater accuracy may be achieved by retaining terms in the kinetic equations up to second order, i.e., Δ^2, c_p^2, and $c_p\Delta$. The solution of these second-order equations is written as the sum of the first-order solution, as already obtained, plus a second-order correction. This sum is substituted into the equations and the second-order correction is then obtained. In practice, the higher the order of terms retained, the greater is the complexity of the equations to be solved. Because the first-order term may easily be sufficiently accurate, there is often very little advantage to extending the solution to second order or beyond.

In applying perturbation methods, we will consider only small deviations in the concentrations of all species from their initial values, i.e., we are concerned with the beginning of the reaction. At time $t = 0$, we assume that no polymers are present, so that $c_p = \Delta = 0$. (The case of nonzero initial conditions has interesting applications and will be discussed in the Further Applications section). Since c_p and Δ are small for short times, we expand the concentration of homogeneous nuclei c_i in a Taylor series in terms of Δ about its initial value $c_{i,0}$, so that we have

$$c_i = c_{i,0} - \left(\frac{\partial c_i}{\partial c}\right)_0 \Delta + \frac{1}{2}\left(\frac{\partial^2 c_i}{\partial c^2}\right)_0 \Delta^2 - \cdots . \tag{9}$$

Similarly, we expand Q about Q_0. If we then substitute these expansions into Eqs. 2 and 8, grouping terms of like order in Δ, we obtain a system of equations that has the form

$$\frac{dc_p}{dt} = a_0 + a_1\Delta + a_2\Delta^2 + \cdots \tag{10a}$$

$$\frac{d\Delta}{dt} = c_p(b_0 + b_1\Delta + b_2\Delta^2 + \cdots). \tag{10b}$$

In the perturbation approach, the lowest-order equation is solved first to obtain the lowest-order approximation to the unknown variables. These lowest-order solutions can then be substituted into the next order set of equations to obtain corrections to the variables. The procedure can be repeated to higher orders until the desired accuracy is obtained. For this reason, it is convenient to write Δ and c_p as a sum of successive approximations

$$\Delta = \Delta_1 + \Delta_2 + \Delta_3 + \cdots \tag{11a}$$

$$c_p = c_p^{(1)} + c_p^{(2)} + c_p^{(3)} + \cdots , \tag{11b}$$

where $\Delta_1 \gg \Delta_2 \gg \Delta_3 \gg \cdots$ and $c_p^{(1)} \gg c_p^{(2)} \gg c_p^{(3)} \gg \cdots$. For this procedure to be valid, it is necessary that $\Delta_1 \ll c_0$ and $c_p^{(1)} \ll c_0$. In addition, it is necessary that a_0 be appropriately small. This will be true whenever the concentration of homogeneous nuclei is small relative to the initial monomer concentration. Since Δ_1 and $c_p^{(1)}$ are both of first order in smallness, the product $c_p^{(1)}\Delta_1$ is of second order, and thus terms containing this quantity should not be included in the first-order equations. With these considerations, the first- or lowest-order equations can be obtained from Eqs. 10 as

$$\frac{dc_p^{(1)}}{dt} = a_0 + a_1\Delta_1 \tag{12a}$$

$$\frac{d\Delta_1}{dt} = c_p^{(1)} b_0, \tag{12b}$$

where, from Eqs. 2 and 8

$$a_0 = k_+ K_i c_0^{i+1} \tag{13a}$$

$$a_1 = k_+[Q_0 - (i+1)K_i c_0^i] \tag{13b}$$

$$b_0 = k_+(c_0 - c_s). \tag{13c}$$

The solutions of Eqs. 12 can be obtained by standard methods and are given by

$$c_p^{(1)} = \frac{a_0}{\sqrt{a_1 b_0}} \sinh \sqrt{a_1 b_0}\, t \tag{14a}$$

$$\Delta_1 = \frac{a_0}{a_1}(\cosh \sqrt{a_1 b_0}\, t - 1) \equiv A(\cosh Bt - 1). \tag{14b}$$

We have introduced some useful shorthand here by defining $A = a_0/a_1$ and $B = \sqrt{a_1 b_0}$. In fundamental terms these are

$$A = \frac{K_i c_0^{i+1}}{(Q_0/k_+) - (i+1)K_i c_0^i} \tag{15a}$$

$$B = k_+ \sqrt{(c_0 - c_s)[(Q_0/k_+) - (i+1)K_i c_0^i]}. \tag{15b}$$

Note that these solutions are independent of the form taken by Q_0 and can thus be used as descriptions of secondary growth, secondary nucleation, or polymer fragmentation. The only limitation is that B must be real, i.e., $a_1 b_0 > 0$. This, in turn, requires that Q_0 be larger than $(i+1)K_i c^i$. This is not a severe limitation, but rather designates a limit below which the form of the solution changes from cosh to cos. (See the Accuracy of the Expansion section).

It is interesting to consider the two limiting forms for the solution Δ_1 (Eq. 14b) that emerge for small and large Bt. For $Bt \ll 1$, we obtain quadratic behavior, namely,

$$\Delta_1 \rightarrow \tfrac{1}{2} B^2 A\, t^2. \tag{16}$$

In this limit, the homogeneous nucleation process dominates over the secondary process, and it is this limit, in fact, that is seen in Oosawa's formulation of homogeneous nucleation and linear polymerization (8, 13). On the other hand, when $Bt \gg 1$, exponential behavior results, namely,

$$\Delta_1 \rightarrow \tfrac{1}{2} A e^{Bt}. \tag{17}$$

In this limit, the secondary process dominates over the homogeneous process to produce this exponential autocatalytic behavior.

The parameters A and B have simple interpretations. A governs the apparent shape of a progress curve, while B, which is an effective rate, sets the time scale of polymerization. For values of A that are small compared with $c_0 - c_s$, it is possible for the solution to reach large values of Bt and still retain reasonable accuracy. This is because the solution itself is limited to the region where Δ_1 is small compared with $c_0 - c_s$. Hence, it is for small values of A that exponential growth can be observed. This is seen in Fig. 1 *a*. For small A, the progress curves appear to increase slowly until some apparent delay time after which the curves turn upward rapidly. Note that once A is sufficiently small to give rise to exponential behavior, changes in A or B will appear to shift the curve along the time axis without altering its shape above the axis. Thus, such a curve can be characterized by its "delay time," as has been done in the study of sickle hemoglobin polymerization. As A becomes large, our solution is restricted to small values of Bt and, consequently, only the parabolic part is observed. As can be seen in Fig. 1 *b*, this increase in A is accompanied by a decrease in apparent delay time. In fact, for these cases, it is difficult to define a delay time at all. Finally, we note that all the curves of our solution begin with t^2 behavior, so that if exponential progress curves were observed with sufficiently high sensitivity near the origin, a parabola should be observed.

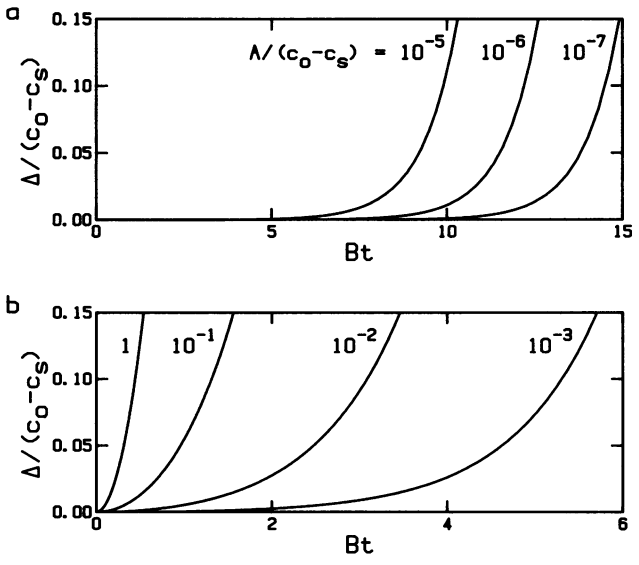

FIGURE 1 Fractional extent vs. time for several values of A. Here, fractional extent $f = \Delta/(c_0 - c_s)$ and time is measured in units of Bt. (*a*) $A/(c_0 - c_s) = 10^{-5}, 10^{-6}, 10^{-7}$, from left to right, respectively. For these small values of A, the apparent delay time, followed by exponential growth, is most clearly demonstrated. As A decreases, these curves appear to shift to longer times without altering their shapes above the axis. (*b*) $A/(c_0 - c_s) = 1, 0.1, 0.01, 0.001$, from left to right, respectively. The curve for $A/(c_0 - c_s) = 1$ is approximately parabolic, and as A decreases, the shape of the curve begins to develop an apparent "delay time," followed by a rapid upward curvature, so that by the value $A = 0.001$, the shape is like that of Fig. 1 *a*.

The advantage of using the first-order perturbation solution to analyze experiments lies in the simplicity of the expressions in Eqs. 14. Analysis of the kinetics of polymerization can yield two parameters, A and B, which can be analyzed in terms of specific models. In particular, since the nature of Q has been unspecified in this solution, it would be of interest to collect a set of A and B, and thus determine the concentration dependence of Q, thereby selecting among the various possible secondary mechanisms.

We also find an extremely useful result if we consider the product B^2A $(=a_0b_0)$. Substituting from Eqs. 13, we find that

$$B^2A = k_+^2(c_0 - c_s)K_ic_0^{i+1}. \tag{18}$$

This result is also independent of Q and contains terms due only to homogeneous nucleation. Hence, it is possible to obtain important information about the homogeneous nucleation step, such as the size of the nucleus, independent of the exact way the secondary process has been modeled, and despite the size of the secondary terms.

ACCURACY OF THE EXPANSION

By the nature of the perturbation approach we have adopted, the first-order solutions are only aproximations that approach the true solution most closely at the start of the reaction. In this section we develop quantitative criteria for assessing the accuracy of the lowest-order solutions. Our first criterion is that $c_p^{(1)}$ and Δ_1 be appropriately small, i.e., $c_p^{(1)} \ll c_0$ and $\Delta_1 \ll c_0$. We also require that our expansions (e.g., Eq. 9) have small higher order terms, which leads to the conditions

$$i\Delta_1 \ll c_0 \tag{19a}$$

$$\left(\frac{\partial Q}{\partial c}\right)_0 \Delta_1 \ll c_0. \tag{19b}$$

From Table I, it is clear that, for fragmentation or lateral growth, the condition, Eq. 19a, is more restrictive than Eq. 19b; however, for heterogeneous nucleation, that condition becomes $j\Delta_1 \ll c_0$, where j is the heterogeneous nucleus size. A priori, it is not clear whether i or j must be larger, and hence pose the more restrictive condition. Roughly speaking, the quantity Δ_1/c_0 reflects the accuracy of the solution, so that, for example, for 1% of the monomers incorporated into polymers, the solution for Δ_1 is accurate to the level of 1%.

We can obtain a better estimate of the accuracy of the solution by solving Eq. 10 to second order, and comparing the size of that term with the size of the first-order term. Including second-order terms in Eq. 10, we have

$$\frac{dc_p}{dt} = a_0 + a_1\Delta + a_2\Delta^2 \tag{20a}$$

$$\frac{d\Delta}{dt} = c_p(b_0 + b_1\Delta), \tag{20b}$$

and we now use

$$\Delta = \Delta_1 + \Delta_2 \tag{20c}$$

$$c_p = c_p^{(1)} + c_p^{(2)}. \tag{20d}$$

The new coefficients needed for second order are simply

$$a_2 = \left(\frac{\partial c_i}{\partial c}\right)_0 + \frac{1}{2}c_0\left(\frac{\partial^2 c_i}{\partial c^2}\right)_0 - \left(\frac{\partial Q}{\partial c}\right)_0$$

$$= \frac{1}{2}i(i+1)K_i c_0^{i-1} - (\partial Q/\partial c)_0 \tag{21a}$$

$$b_1 = -k_+. \tag{21b}$$

The solutions $c_p^{(2)}$ and Δ_2 are the second-order terms in the expansions of c_p and Δ. The term Δ_2 is of greatest interest here; it is found to be

$$\Delta_2 = \frac{a_0^2 b_0}{(a_1 b_0)^3}\left[\frac{3}{2}a_2 b_0^2(\cosh\sqrt{a_1 b_0}\,t - 1)\right.$$

$$-\frac{1}{2}(2a_2 b_0^2 + a_0 b_0 b_1)\sqrt{a_1 b_0}\,t\sinh\sqrt{a_1 b_0}\,t$$

$$+\frac{1}{3}\left(\frac{1}{2}a_2 b_0^2 + a_0 b_0 b_1\right)(\cosh 2\sqrt{a_1 b_0}\,t$$

$$\left.-\cosh\sqrt{a_1 b_0}\,t)\right]. \tag{22}$$

In general, this full expression must be used to ascertain the size of the second-order term. The new parameters that appear in the second-order solution, a_2 and b_1, can be calculated once the analysis of the first-order solution is complete. This provides a better estimate of the error incurred in using the first-order solution than the inequalities presented at the beginning of this section. A detailed example of the use of such measures of accuracy is presented in the Actin section.

As noted above, the hyperbolic cosine solution given by Eq. 14b requires that a_1 be positive. When a_1 is negative (i.e., when $Q_0 < [i+1]K_i c^i$), the argument Bt becomes imaginary. This is equivalent to a cosine solution of real argument and gives us

$$\Delta_1 = A(\cos|B|t - 1), \tag{23}$$

where we have used the definitions of Eqs. 15 a, b. The oscillatory nature of the cosine never appears. When A is large, the approximations leading to this solution break down as $|B|t$ becomes large. When A is small (e.g., i large), we use Eq. 19a and find

$$1 - \cos|B|t \ll 1 + \frac{1}{i}. \tag{24}$$

This restricts the solution with $B^2 < 0$ to the small $|B|t$ limit in all cases, i.e.,

$$\Delta_1 = \tfrac{1}{2}B^2 A\,t^2, \tag{25}$$

since for small magnitude of Bt, the higher orders contribute little to the cosine.

ACTIN

In the presence of salts, F-actin assembles into double-stranded helical polymers (18). Actin polymerization has long been thought to exemplify nucleation-controlled polymerization (1, 8). Recently, Wegner and Savko have proposed that under certain solution conditions, the homogeneous nucleation process is augmented by fragmentation of actin polymers (9, 10). Although evidence for fragmentation does not come solely from the assembly kinetics, the kinetics do clearly demonstrate the inadequacy of simple homogeneous nucleation, and the numerical simulations of Wegner and Savko show that a fragmentation model can recitify the discrepancies.

In this section, we reexamine the data of Wegner and Savko using our perturbation method. Our results, though similar to theirs, are not identical. More importantly, however, the results obtained for the homogeneous process do not depend on the secondary process. Previous analysis has been criticized on the basis that the modeling of polymerization with fragmentation makes the choice of a nucleus size less reliable than if fragmentation were absent (19).

We begin the analysis by examining the data taken under the conditions most favorable to the secondary process, namely, polymerization in the presence of 0.6 mM MgCl and 0.5 mM EGTA. For seven different actin concentrations between 6.7 and 22.9 μM, polymerization was followed by measuring light scattering as a function of time. (See Fig. 7 of reference 10.) Because the perturbation solution is an approximation, only the initial portion of the progress curves can be analyzed in this way. As a guide to determining how much of the progress curve should be analyzed, we need to consider the scatter in the experimental data. Roughly speaking, we can allow the perturbation solution to be inaccurate by the same amount as the data scatters. The inaccuracy we tolerate in the solution, in turn, is reflected in the fraction of the curve analyzed. Because the scatter of the data is of the order of 15%, we choose to analyze only the first 15% of the data. Once we have obtained fits to the data, we then must determine whether the size of the second-order terms exceeds this figure of merit.

To account for the fact that the second-order correction is largest at the highest data points, we ascribed an error to each point proportional to the magnitude of the point itself and added that error to the intrinsic digitization error (see below). This procedure was used to assure that the fit was weighted more strongly by the points where the first-order solution has greatest accuracy. Such an approach is justi-

fied by the fact that, in perturbation theory, the second-order term, Δ_2, is of order Δ_1^2, the third-order term, Δ_3, is of order Δ_1^3, etc.

Because of our need to focus on the initial portion of the progress curves, precise background subtraction is important. The data from Wegner's study contain a digitization step, i.e., all concentrations in the recorded progress curves are multiples of some finite value. Hence, background subtraction may be in error by plus or minus one such step. Consequently, we included in our fits a term for a constant offset; however, we restricted this term to be less than or equal to one digitization step. In most data sets, the offset term was fit within the restriction. When the offset was not included, only small differences in the results were found, which do not affect the major conclusions below. We also used this digitization step size as a convenient measure of error to be added to the error ascribed above.

We fit the solution of Eq. 14b to the first 15% of Wegner and Savko's data using a standard iterative nonlinear least-squares fitting routine (20). Two such data sets with the resulting fits are shown in Fig. 2. As expected from the success of numerical integrations, Eq. 14b describes the data quite well. The compilation of all the fitted parameters is given in Table II. We note that A is, in general, quite small relative to $(c_0 - c_s)$. Thus we find the $\cosh(Bt)$ ranging from t^2 to the exponential limit.

In Fig. 3, we plot $\log[A/(c_0 - c_s)]$ and $\log(B)$ vs. $\log(c_0)$. As can be seen, A is much more strongly concentration dependent than B. With a threefold change in concentration, A increases by almost two decades, while B increases by only about one decade. Moreover, half the increase in B occurs between the first two points, so that for most of the data B exhibits little change.

From the values of A and B, we can determine the constants of the polymerization process. We first examine B^2A, since it contains terms solely due to homogeneous nucleation. A plot of $\log\{B^2A/[c_0(c_0 - c_s)]\}$ vs. $\log(c_0)$ gives the nucleus size directly, since

$$\log\{B^2A/[c_0(c_0 - c_s)]\} = \log(k_+^2K_i) + i\log c_0. \quad (26)$$

As can be seen, this has a simple linear behavior in $\log(c_0)$, and the slope of that line is the nucleus size i. The intercept gives the product $k_+^2K_i$. In Fig. 4, we have constructed such a plot for the data shown in Fig. 3. The solid line shows a linear least-squares fit, which gives a nucleus size $i = 2.92 \pm 0.11$ and $\log(k_+^2K_i) = -4.23 \pm 0.13$. The dashed line shows the best-fit line with a nucleus size of 4, as used by Wegner and Savko. Although it does not give the best representation of the data, it does fit a portion of the data.

Once homogeneous nucleation has been parameterized, the nature of the secondary process remains to be determined. It is the concentration dependence of Q_0 that permits us to distinguish between the various models. From the data we can only determine the product k_+Q_0. This is equivalent to examining Q_0 alone since k_+ is concentration independent. (This analysis will not separately determine k_+ unless the number of polymers as a function of time is known.) Only the parameters A and B and the nucleus size

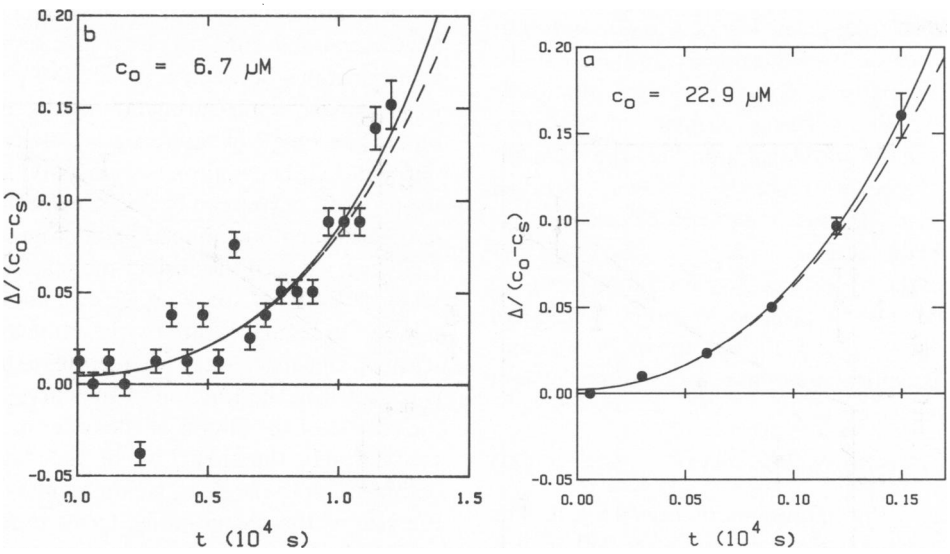

FIGURE 2 Fractional extent vs. time for actin polymerization in the presence of 0.6 mM mgCl and 0.5 mM EGTA. Fractional extent is defined as $f = \Delta/(c_0 - c_s)$, and time is expressed in units of 10^4 s. Initial actin monomer concentrations are (*a*) $c_0 = 22.9$ μM and (*b*) $c_0 = 6.7$ μM. Solid dots are actual data points of Fig. 7 of Wegner and Savko (reference 10). The error bars on these points are obtained by adding the digitization step size to Δ_1^2, the estimated error in the first-order perturbation solution Δ_1. Digitization step size for (*a*) was 0.0698 and for (*b*) was 0.0595. The solid curves are the theoretical curves calculated using the first-order solution Δ_1 (Eq. 14b), which were fit to the data to determine A and B. (See Table II.) The dashed curve is the sum of this solid curve and the second-order correction to the solution Δ_2 (Eq. 22). In calculating Δ_2, we use the values of A and B from the first-order fit and we assume fragmentation (i.e., that Q is constant). The cases shown here are two extremes; other fits do not differ significantly. Parameters are tabulated in Table II.

TABLE II
ACTIN ANALYSIS

$c_0(\mu M)$	No. of points	$A/(c_0 - c_s)$	$B(10^{-4}s^{-1})$	D(digits)	χ^2	(Δ_2/Δ_1) max
Magnesium (c_s = 2.0 μM)						
6.7	21	0.035 ± 0.018	1.86 ± 0.36	0.37 ± 0.18	8.4	−0.11
8.5	15	0.0041 ± 0.0013	4.97 ± 0.40	1.00*	4.1	−0.11
11.5	10	0.0119 ± 0.0040	6.26 ± 0.65	0.71 ± 0.27	8.1	−0.13
14.9	11	$B^2A/(c_0 - c_s)$ = 3.017 ± 0.070‡		1.00*	4.5	—
17.3	9	0.034 ± 0.010	10.3 ± 1.2	0.47 ± 0.30	3.3	−0.11
20.3	7	0.097 ± 0.044	8.5 ± 1.7	−0.51 ± 0.33	1.2	−0.094
22.9	6	0.090 ± 0.042	11.1 ± 2.3	0.67 ± 0.35	1.8	−0.096
Calcium (c_s = 2.0 μM)						
6.9	27	0.0076 ± 0.0021	2.40 ± 0.19	1.00*	7.6	—
9.4	15	0.033 ± 0.016	2.65 ± 0.48	0.73 ± 0.22	15.0	—
11.7	8	$B^2A/(c_0 - c_s)$ = 1.672 ± 0.053‡		1.00*	8.5	—
15.1	6	$B^2A/(c_0 - c_s)$ = 3.92 ± 0.13‡		1.00*	11.4	—
17.7	4	$B^2A/(c_0 - c_s)$ = 12.07 ± 0.44‡		1.00*	31.1	—
20.1	3	$B^2A/(c_0 - c_s)$ = 21.7 ± 1.0‡		0.98 ± 0.46	28.8	—
24.1	3	$B^2A/(c_0 - c_s)$ = 6.20 ± 2.8‡		0.53 ± 0.47	19.7	—
Potassium (c_s = 1.5 μM)						
7.4	13	$B^2A/(c_0 - c_s)$ = 0.585 ± 0.025‡		0.87 ± 0.22	14.9	—
9.6	6	0.0260 ± 0.0072	7.74 ± 0.77	−0.56 ± 0.29	2.7	—
12.4	4	$B^2A/(c_0 - c_s)$ = 8.12 ± 0.32‡		−1.00*	13.5	—
14.2	6	$B^2A/(c_0 - c_s)$ = 12.16 ± 0.37‡		1.00*	24.5	—
16.2	4	$B^2A/(c_0 - c_s)$ = 28.25 ± 0.98‡		1.00*	18.7	—
18.4	4	$B^2A/(c_0 - c_s)$ = 23.3 ± 1.1‡		−0.03 ± 0.37	1.5	—
20.5	3	$B^2A/(c_0 - c_s)$ = 66.5 ± 3.1‡		0.81 ± 0.45	24.8	—

The digitization errors for magnesium are the following: 0.0595, 0.0603, 0.0603, 0.0599, 0.0599, 0.0698, 0.0698; for calcium, 0.0647, 0.0647, 0.0647, 0.06388, 0.0638, 0.0653, 0.0759; and for potassium, 0.062, 0.062, 0.062, 0.06298, 0.0611, 0.0759, 0.0611.
*Set to 1.00.
‡Parabolic approximation.

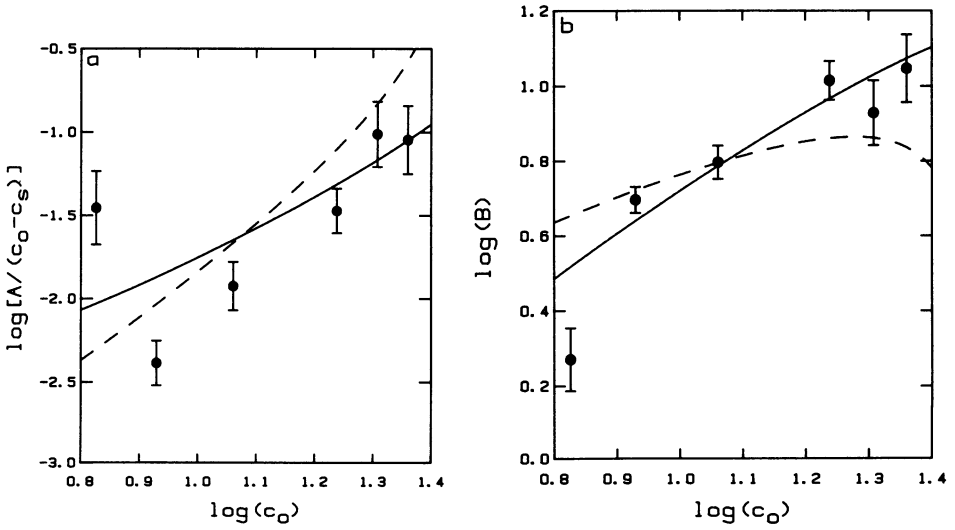

FIGURE 3 Dependence of A and B on initial monomer concentration c_0 for actin polymerization in the presence of magnesium, with c_0 in micromoles per liter. The values of A and B, listed in Table II, were obtained by fitting the first-order perturbation solution Δ_1 (Eq. 14b) to approximately the first 15% of the data of Fig. 7 of Wegner and Savko (reference 10). Points are plotted, with their respective fitting errors, for each progress curve for which A and B could be determined independently. The solid curves are the theoretical curves for A and B calculated by using a power law dependence for Q_0 obtained from Fig. 5, and the dashed curves are the dependences obtained by assuming that Q_0 is the

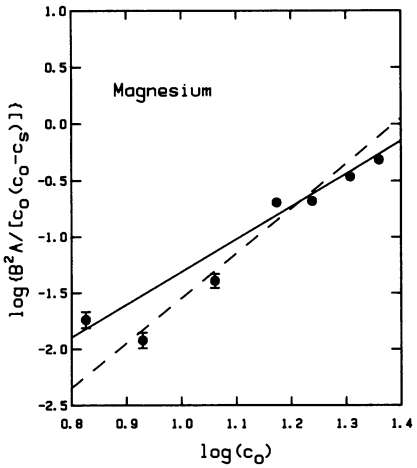

FIGURE 4 Determination of homogeneous nucleation parameters for actin polymerization in the presence of magnesium. This log-log plot of B^2A, scaled by $c_0(c_0 - c_s)$, vs. c_0 in μM, yields the homogeneous nucleus size i and rate parameter $k_+^2K_i$. Data points correspond to the points for A and B in Fig. 3 and listed in Table II, and the error bars were determined by fitting Δ_i (Eq. 14b) to the data using the parameters B^2A and B (instead of A and B). For the four highest data points, the error bars are smaller than the dots. The solid line is a least-squares fit to the points and yields a nucleus size $i = 2.92 \pm 0.11$ from the slope and $\log(k_+^2K_i) = -4.23 \pm 0.13$ from the intercept. (See Eq. 26.) The dashed line is a best fit line with a nucleus size of 4, as used by Wegner and Savko. Note that this does fit a portion of the data.

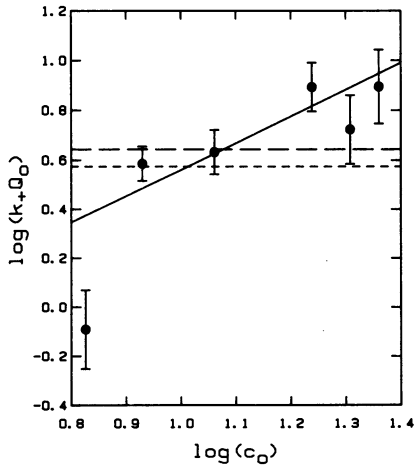

FIGURE 5 Determination of the nature of the secondary process: concentration dependence of Q_0, scaled with k_+, with c_0 in micromoles per liter. k_+Q_0 is calculated with values of A and B from Fig. 3, listed in Table II, with nucleus size i from Fig. 4, and with the use of Eq. 27. The long dashes represent the best-fit constant through the data, $\log(k_+Q_0) = 0.463 \pm 0.042$, and the short dashes represent the constant used by Wegner and Savko, $\log(k_+Q_0) = 0.547$. The solid line is the best-fit line, with a slope of 1.07 ± 0.25 and an intercept of -0.51 ± 0.27. Constant Q_0 appears when the secondary mechanism is fragmentation, while a slope of unity is the result of lateral growth. Heterogeneous nucleation can be ruled out.

i are needed to determine k_+Q_0, which, from Eqs. 15, is given by

$$k_+Q_0 = [B^2 + (i + 1)(B^2A/c_0)]/(c_0 - c_s). \quad (27)$$

In Fig. 5, we plot $\log(k_+Q_0)$ vs. $\log(c_0)$. Despite considerable scatter, Q_0 does seem to increase with increasing c_0. For pure fragmentation we expect to find a constant $Q_0(= k_{fr})$. If we fit the data of Fig. 5 with a constant (equivalent to taking the average weighted by errors), we get $\log(k_+Q_0) = 0.643 \pm 0.042$, which is close to the value of 0.574 obtained by Wegner and Savko. Our average is shown in Fig. 5 as the long dashes; that of Wegner and Savko is shown by the short dashes.

If we assume that the data are scattered about a straight line, we obtain a slope of that line of 1.07 ± 0.25 and an intercept of -0.51 ± 0.27. If the secondary process were lateral growth, we would expect to have a slope of unity; if the secondary process were heterogeneous nucleation, the slope would give the nucleus size. Thus, with a slope of 1.07, heterogeneous nucleation is unlikely as a source of the secondary process but, based on purely kinetic analysis, lateral growth cannot be excluded. In fact, from kinetic analysis alone, one would be forced to conclude that the secondary process is lateral growth. Even if the lowest data point is excluded from the analysis, the slope remains significantly different from zero (0.72 ± 0.27). However, it is clear that the scatter in the kinetic data weakens the distinction between lateral growth and fragmentation, and points to the necessity of gathering precise data at the beginning of the progress curves to take full advantage of the strength of this method.

From the preceding analysis, we can calculate theoretical curves for A and B. These are shown in Fig. 3. For the solid curves, we have assumed a nonzero slope (see above), while for the dashed curves we have assumed strict fragmentation and hence constant Q_0. We note that when Q_0 is constant, B is nearly constant for a considerable range. This result arises from the dominance of Q_0 in the expression for B, indicating that the secondary process dominates. This is actually readily apparent from the smallness of A. (See Eq. 15a.) In such a situation, note that B and B^2A then independently describe the secondary process and the homogeneous nucleation step, respectively.

Once the first-order fitting procedure is complete, we may compute the second-order term to verify that the expected accuracy of our solution is satisfied. Contained in the second-order term is the concentration dependence of Q. (See Eq. 21a.) For computing the size of the second-order term, we have assumed that Q arises from fragmentation, and thus has no concentration dependence. In Table II, we list the maximum ratio of second order to first order. As expected, all are at approximately the 10% level. In Fig. 2, we have plotted the sum of the first- and second-order solutions. The second-order correction begins quite small, and its contribution is only apparent near the point at which we have chosen to truncate the curve. (In fact, it can be demonstrated that the second-order term will have terms of no lower power than t^4.) The second-order term

does not change by much if we use the lateral growth model instead (i.e., Q proportional to c).

Wegner and Savko also studied actin polymerization in the presence of calcium and potassium. They found that some fragmentation was required to fit the data for calcium, whereas none was required for the potassium data. We attempted to analyze these data sets by the same method as we employed for the magnesium data above. For the calcium data, only two of the seven curves produced a convergent fit using the cosh function. This mainly results from the failure of the secondary process, represented by Q, to compete effectively with homogeneous nucleation. When the latter dominates, the perturbation solution is restricted to the small Bt limit, and hence t^2 behavior. In fact, if we fit the data with a power series in even powers (as the model requires), we find that the t^2 term dominates, and the t^4 term is indistinguishable from zero within the errors of the fit. (Note that in several curves, very few points were available for analysis.) In short, the initial data were not sufficiently precise to extract more than the coefficient of a single power of time.

Data that could not fit to a cosh were fit to a parabola, and this gave the B^2A product directly. (Only B^2A contributes to the t^2 term, even if higher order perturbation terms are included.) The results of the parabolic fits are also given in Table II. Fig. 6 shows B^2A plotted for the calcium data as a function of concentration. We find this log-log plot to be linear with a nucleus size $i = 4.66 \pm 0.11$, and with $\log(k_+^2 K_i) = -6.00 \pm 0.12$. For this data, Wegner used a nucleus size of 4. Such a line is drawn as the dashed line in Fig. 6. Fig. 7 shows B^2A for the potassium data. We find a good linear fit again, with a nucleus size $i = 3.54 \pm 0.13$, and with $\log(k_+^2 K_i) = -4.14 \pm 0.15$. Wegner employed a nucleus of 3, drawn as the dashed line.

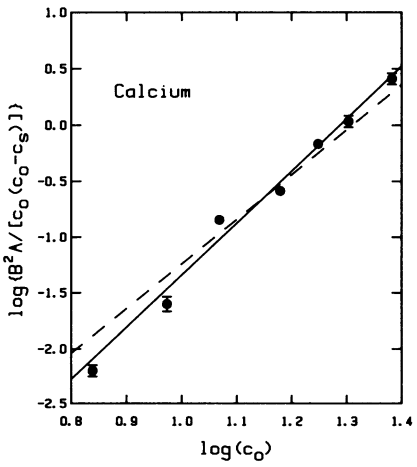

FIGURE 6 Determination of homogeneous nucleation parameters for actin polymerization in the presence of calcium. This plot is analogous to Fig. 4, where here the data is from Fig. 6 of Wegner and Savko (reference 10), and the nucleus size is $i = 4.66 \pm 0.11$, with $\log(k_+^2 K_i) = -6.00 \pm 0.12$. The nucleus size for the dashed line is 4, as used by Wegner and Savko. The error bars were determined as in Fig. 4. They are smaller than the dots for the middle three data points.

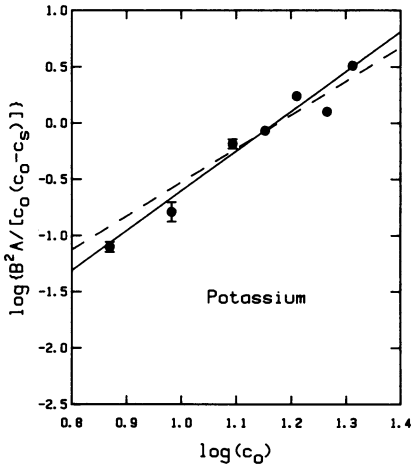

FIGURE 7 Determination of homogeneous nucleation parameters for actin polymerization in the presence of potassium. This is analogous to Figs. 4 and 6, where here the data is from Fig. 5 of Wegner and Savko (reference 10), and the nucleus size is $i = 3.54 \pm 0.13$ and $\log(k_+^2 K_i) = 4.14 \pm 0.15$. The nucleus size for the dashed line is 3, as used by Wegner and Savko. Error bars were determined as in Figs. 4 and 6. As in Fig. 6, they are smaller than the dots for the middle three data points.

In addition to illustrating the use of the perturbation procedure, this analysis makes several points. (*a*) Wegner's numerical approach and this analytic method agree best when the secondary process is weakest. This supports the contention of Tobacman and Korn (19) that such a process of numerical integration with several variables makes nucleus determination difficult. (*b*) Lateral growth formally describes the data better than fragmentation. (Equivalently, there is a concentration dependence to the fragmentation term.) (*c*) The nucleus size varies with the nature of the salt. This last conclusion was anticipated by Wegner and Savko. We have extended that analysis allow for noninteger nuclei.

COLLAGEN

The assembly of collagen fibers involves a number of steps by which parallel arrays of microfibrils are thought to be assembled, each of which is itself a fivefold helix of collagen molecules (21). At present, there is no consensus in the literature as to whether assembly of collagen fibers involves a nucleation step, and it is not our purpose here to answer that question (11, 12, 22–25). We wish to show the behavior of a system with known lateral aggregation, when analyzed by our perturbation method. For simple nucleation and growth Oosawa (1, 8) has shown that the nucleus size can be obtained from the slope of a plot of log of characteristic time vs. log concentration. In this section, we show that in the presence of augmented nucleation such a procedure can dramatically fail to find the nucleus size.

We wish to consider the implications of a secondary

process that is much more favorable than continued nucleation. In this case, $Q_0 \gg k_+(i+1)K_i c_0^i$, and so we find

$$A \simeq \frac{k_+ K_i c_0^{i+1}}{Q_0} \tag{28a}$$

and

$$B \simeq \sqrt{k_+(c_0 - c_s)Q_0}. \tag{28b}$$

For lateral growth, $Q_0 = k_+' c_0$. If we consider $c_0 \gg c_s$, which appears to be true for collagen, we find that B is simply proportional to c_0, and A is proportional to c_0^i.

Polymerization reactions are often characterized by the time required to reach a specific fractional extent. If we consider the exponential growth limit, we find that the time at which a given fractional extent F is reached is given by

$$t_F = \frac{1}{B} \ln \frac{2F(c_0 - c_s)}{A}. \tag{29}$$

The time to reach a given extent depends most strongly on B, since A appears in a logarithm. Thus the concentration dependence of t_F will primarily reflect the concentration dependence of B, and only weakly reflect the concentration dependence of A. For the case of lateral growth considered above

$$\frac{\partial \log t_F}{\partial \log c_0} \simeq -1. \tag{30}$$

For homogeneous nucleation and growth without a secondary pathway, the concentration dependence of t_F is related to the nucleus size. As Oosawa (1, 8) has shown, for such a case,

$$\frac{\partial \log t_F}{\partial \log c_0} = -\frac{(i+1)}{2}. \tag{31}$$

Consequently, the analysis of nucleation augmented by lateral growth by using methods designed to analyze homogeneous nucleation alone would imply that the nucleus size was unity (i.e., no nucleation). Hence, the slope of a plot of $\log(t_F)$ vs. $\log(c_0)$ will yield the homogeneous nucleus size only in the absence of a secondary process. Conversely, a laterally growing polymerization process could seem devoid of nucleation in an Oosawa-type analysis even though a nucleation step may well be present. As we have described above, the homogeneous nucleus size may always be determined correctly by analysis of the concentration dependence of B^2A, regardless of the presence or absence of a secondary pathway.

FURTHER APPLICATIONS

Degree of Polymerization

Once Δ_1 and $c_p^{(1)}$ are known, we can develop a simple expression for the average degree of polymerization, $\langle n \rangle$. From Eqs. 14, we find

$$\langle n \rangle \equiv \frac{\Delta}{c_p} = \frac{b_0(\cosh Bt - 1)}{B \sinh Bt}. \tag{32}$$

For small Bt, we have $\langle n \rangle \simeq b_0 t/2$. This physically describes the fact that at the initial time, the average polymer length increases linearly. At large Bt, we have the surprising result that $\langle n \rangle$ becomes constant, i.e., we get $\langle n \rangle = b_0/B$. This, of course, only applies during the exponential growth phase. This result says that new polymer formation is matched by polymer growth. The fact that these match exactly is built in by our assumption that the secondary process is proportional to the concentration of incorporated monomers.

Polymer Parentage

We can also ask how many polymers form by each pathway. We denote the concentration of polymers formed by homogeneous nucleation as c_p', while polymers formed by the secondary process will be labeled c_p''. We need to separate the terms in Eqs. 8 and 12. For convenience, we define the coefficient of Δ_1 in the homogeneous nucleation term as

$$a_1' \equiv -k_+(i+1)K_i c_0^i, \tag{33}$$

so that $a_1 = a_1' + k_+ Q_0$. We then have (to first order) the decoupled differential equations for polymer formation via each pathway, namely

$$\frac{dc_p'}{dt} = a_0 + a_1' \Delta_1 \tag{34a}$$

$$\frac{dc_p''}{dt} = k_+ Q_0 \Delta_1. \tag{34b}$$

These have the solutions

$$c_p' = a_1'(A/B) \sinh Bt + k_+ Q_0 At \tag{35a}$$

$$c_p'' = k_+ Q_0 (A/B) \sinh Bt - k_+ Q_0 At. \tag{35b}$$

These equations behave quite differently because a_1' must be negative, whereas Q_0 is positive. Thus, the concentration of homogeneously formed polymers c_p' will rise and saturate, while c_p'', the secondarily formed polymers, will grow exponentially. Again, these results are restricted to the initial phase of the reaction. Thus the secondary process will come to dominate the formation of polymers. We can express the fraction of polymers formed by the secondary pathway as

$$\frac{c_p''}{c_p} = \frac{k_+ Q_0}{a_1}\left(1 - \frac{Bt}{\sinh Bt}\right). \tag{36}$$

The function in brackets is shown in Fig. 8. As can be seen, at roughly 5 Bt this saturating function has reached 90%.

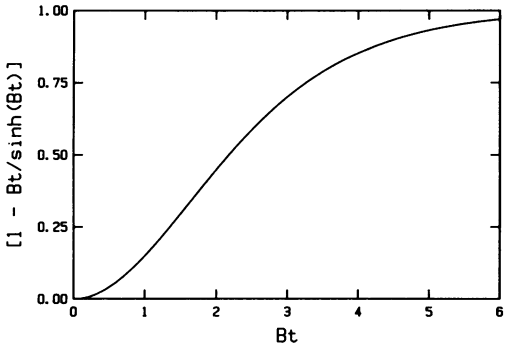

FIGURE 8 Time dependence of the fraction of polymers formed by the secondary pathway. $[1 - Bt/\sinh(Bt)]$ vs. Bt, as given in Eq. 36, shows how the secondary process comes to dominate polymer formation. At roughly $5Bt$, this saturating function has reached 90%.

Cycling Experiments

This perturbation method is also well suited to analyze cycling or depolymerization-repolymerization experiments. In such experiments, conditions on a polymerized sample are changed to induce depolymerization. Some time later, usually after the disappearance of detectable polymer signal, conditions are restored so as to favor polymerization. The repolymerization is often accompanied by a decreased delay time (26). In this section, we shall analyze such experiments by making the simple assumption that not all polymer has disappeared when repolymerization is initiated, so that we do not begin with zero incorporated monomers or zero polymer concentration. We shall designate the residual concentration of incorporated monomers presented as Δ^*, and the concentration of residual polymer as c_p^*.

We can again write a perturbation expansion. However, we must note that now Δ is the additional amount of polymerized monomer; the total amount of polymerized monomer is $\Delta^* + \Delta$. Likewise, c_p represents the additional concentration of polymer. The rate of monomer incorporation is then

$$\frac{d\Delta}{dt} = (k_+ c - k_-)(c_p + c_p^*). \tag{37a}$$

and the rate of polymer formation is

$$\frac{dc_p}{dt} = k_+ K_i c^{i+1} + Q(\Delta + \Delta^*). \tag{37b}$$

These are in the same form as Eqs. 2 and 8, respectively. We can expand these, as in Eqs. 10. In addition to the conditions imposed there, c_p^* and Δ^* must also be small relative to c_0 for the expansions to converge. We then obtain the first-order equations, analogous to Eqs. 12. These are given by

$$\frac{d\Delta_1}{dt} = b_0 c_p^* + b_0 c_p^{(1)} \tag{38a}$$

$$\frac{dc_p^{(1)}}{dt} = a_0^* + a_1 \Delta_1. \tag{38b}$$

We used a^* to show the similarity between these equations and Eqs. 12. The relationship between a_0^* and a_0 is just

$$a_0^* = a_0 + Q_0 \Delta^*. \tag{39}$$

The solution to Eqs. 38 is somewhat more complicated than that found for Eqs. 12; however, there are a number of useful simplifications that emerge. The full first-order solution is

$$\Delta_1 = (A + \Delta^*)(e^{\lambda_0 t}\cosh \lambda_1 t - 1) + \frac{\lambda_0}{\lambda_1}(2(c_0 - c_s) - \Delta^* - A)e^{\lambda_0 t}\sinh \lambda_1 t, \tag{40a}$$

where

$$\lambda_0 \equiv k_+ c_p^*/2 \tag{40b}$$

and

$$\lambda_1 \equiv \sqrt{\lambda_0^2 + B^2}. \tag{40c}$$

If the initial concentration of polymers c_p^* is so small that $\lambda_0 \ll \lambda_1$, then Eq. 39a has a particularly simple form, namely,

$$\Delta_1 = (A + \Delta^*)(\cosh Bt - 1). \tag{41}$$

This shows that repolymerization has the same form as the initial polymerization, and in fact, will have the same rate B. However, because $(A + \Delta^*)$ is larger than A, a signal will be observed at an earlier time than found at first, so that the apparent delay time will have shortened. (See Fig. 1.) For exponential growth curves, the repolymerization curve will have the same exponential shape, but will be translated along the time axis, and the shortening of the delay time will be roughly given by

$$\Delta t_d \simeq \frac{1}{B}\ln\frac{A}{\Delta^*}. \tag{42}$$

CONCLUSIONS

We have presented a perturbation method for the analysis of nucleation-controlled polymerization that is augmented by a secondary pathway for polymer growth. Previous methods for analyzing such models have required numerical integration of the kinetic equations, so that finding parameters that give agreement between theory and experiment has been a difficult process. With the perturbation method presented here, the solution to the kinetic equations assumes a simple analytic closed form that can easily be used in fitting data. So long as the formation of polymers by the secondary pathway depends linearly on the concentration of monomers polymerized, the kinetic equations assume the same simple form. This permits the

analysis of augmented growth models with a minimum number of modeling assumptions, and thus makes it readily possible to distinguish between a variety of secondary processes (heterogeneous nucleation, lateral growth, and fragmentation). In addition, the parameters of the homogeneous process, such as the homogeneous nucleus size, can be determined independent of the nature of the secondary mechanism.

The method presented here is limited to the initial phase of the polymerization reaction, and we have shown how the errors incurred depend upon the fractional extent of the reaction that is analyzed. We have shown how this method applies to analysis of actin, collagen, and sickle hemoglobin. In analyzing published actin data, we find that further work is necessary to distinguish between fragmentation and lateral growth on the basis of kinetic data alone.

Because this method is accurate only in the initial phase of polymerization, it is crucial to obtain ample data of high quality at the beginning of the reaction. Techniques such as light scattering or fluorescence are well suited to this task because of their wide dynamic range, in contrast to, say, turbidometric assays, which are more restricted. Data analysis by this method will be greatly assisted by gain setting strategies or logarithmic data collection to obtain as much data as possible in the initial phase.

APPENDIX

Solution Nonideality

Sickle cell hemoglobin is a mutant hemoglobin that can assemble into multistranded polymers (14 or 16 strands) (27, 28), which in turn can form larger arrays of aligned polymers. Heterogeneous nucleation has been proposed as a mechanism to augment the formation of sickle cell hemoglobin polymers by allowing the surface of one polymer to act as a nucleation site for additional polymers (14). Under physiological conditions, the solubility of sickle cell hemoglobin is sufficiently high that polymerization is only seen in highly concentrated solutions. Under such conditions, we can no longer consider the solution ideal in the thermodynamic sense, and we must include activity coefficients in the thermodynamic and kinetic formulation. The nonideality is that of so-called excluded volume (29), and arises to account for the fact that the proximity of the molecules is underestimated by use of concentration along. Here we shall show how nonideality alters the kinetic equations.

The procedure for modifying the differential equations for polymerization is to multiply the ideal rate constant by activity coefficients for the reactants, and divide by the activity coefficient for the activated complex. This changes Eq. 2 into the form

$$\frac{d\Delta}{dt} = (k_+\gamma c - k_-)c_p, \tag{A1}$$

where γ is the activity coefficient for monomers, and is itself a function of concentration. Now k_- is given by $k_+\gamma_s c_s$, where γ_s is the activity coefficient measured at the solubility c_s. Polymer activity coefficients do not appear because we assume that the polymer and the activated complex have the same coefficient, and hence these cancel. For the homogeneous pathway, Eq. 4 becomes

$$\frac{dc_p}{dt} = k_+ \frac{\gamma\gamma_i}{\gamma_i^\ddagger} cc_i, \tag{A2}$$

where the nucleus and the activated complex (of nucleus plus one monomer) have activity coefficients of γ_i and $\gamma_i^\ddagger$, respectively. Rather than attempt to cancel the latter, we make use of the fact that $\gamma_i c_i$ is the activity of the nucleus, which we shall denote as z_i. This quantity can be computed by various thermodynamic treatments, e.g.,

$$z_i = K_i(\gamma c)^i. \tag{A3}$$

As we show elsewhere, this is not entirely analogous for the heterogeneous pathway; there it is useful to cancel the terms for aggregate activity. The resulting equation for polymer formation is thus

$$\frac{dc_p}{dt} = k_+ \frac{\gamma c z_i}{\gamma_i^\ddagger} + \phi k_+ \gamma c c_j (c_0 - c). \tag{A4}$$

Now we proceed as in the First-Order Solution section except that here γ and $\gamma_i^\ddagger$ must be expanded, in addition to the concentrations of all species in solution. Likewise, we will expand z_i. This gives rise to exactly the same form of equations as Eqs. 12, with the coefficients now given by

$$a_0 = \frac{k_+\gamma_0 c_0 z_{i,0}}{\gamma_{i,0}^\ddagger} \tag{A5}$$

$$a_1 = k_+\gamma_0 c_0 \left\{ \phi c_{j,0} - \frac{1}{\gamma_{i,0}^\ddagger}\left(\frac{\partial z_i}{\partial c}\right)_0 + z_{i,0}\left[\frac{1}{c_0} + \left(\frac{\partial \ln(\gamma/\gamma_i^\ddagger)}{\partial c}\right)_0\right]\right\} \tag{A6}$$

$$b_0 = k_+(\gamma_0 c_0 - \gamma_s c_s). \tag{A7}$$

The solutions are then given by Eqs. 14, as before.

Sickle cell hemoglobin can also polymerize in high-phosphate buffers, in which the solubility is sufficiently lowered that nonideality is not a problem (26). For such a case, assuming that the high phosphate does not alter the intermolecular interactions, heterogeneous nucleation is modeled in a straightforward way, without the complications detailed here. A complete analysis of the behavior of sickle hemoglobin polymerization is the subject of a separate paper (Ferrone, F. A., J. Hofrichter, and W. A. Eaton, manuscript in preparation).

We thank Dr. A. Wegner for graciously providing us with a tabulation of his published actin data (10); we thank Dr. A. Szabo for helpful comments regarding our derivation; and we thank Dr. J. Hofrichter for bringing the work on actin to our attention.

We acknowledge the support of the National Heart, Lung, and Blood Institute of the National Institutes of Health (F. A. Ferrone, HL28102; M. F. Bishop, HL31549).

Received for publication 9 January 1984 and in final form 14 June 1984.

REFERENCES

1. Oosawa, F., and M. Kasai. 1962. Theory of linear and helical aggregations of macromolecules. *J. Mol. Biol.* 4:10–21.
2. Butler, P. J. G., and A. Klug. 1971. Assembly of the particle of tobacco mosaic virus from RNA and disks of protein. *Nature New Biol.* 229:47–50.
3. Olmsted, J. B., and G. G. Borisy. 1973. Characterization of microtubule assembly in porcine brain extracts by viscometry. *Biochemistry.* 12:4282–4289.
4. Hofrichter, J., P. D. Ross, and W. A. Eaton. 1974. Kinetics and mechanism of deoxyhemoglobin S gelation: A new approach to understanding sickle cell disease. *Proc. Natl. Acad. Sci. USA.* 71:4864–4868.
5. Malfa, K., and J. Steinhardt. 1974. A temperature-dependent latent period in the aggregation of sickle cell deoxyhemoglobin. *Biochem. Biophys. Res. Commun.* 59:887–893.

6. Steinert, P. M., W. W. Idler, and S. B. Zimmerman. 1976. Self-assembly of bovine epidermal keratin filaments *in vitro*. *J. Mol. Biol.* 108:547–567.
7. Vialtel, P., D. I. C. Kells, L. Pinteric, K. J. Dorrington, and M. Klein. 1982. Nucleation-controlled polymerization of human monoclonal immunoglobulin cryoglobulins. *J. Biol. Chem.* 257:3811–3818.
8. Oosawa, F., and S. Asakura. 1975. Thermodynamics of the Polymerization of Protein. Academic Press, Inc., New York.
9. Wegner, A. 1982. Spontaneous fragmentation of actin filaments in physiological conditions. *Nature (Lond.)* 296:266–267.
10. Wegner, A., and P. Savko. 1982. Fragmentation of actin filaments. *Biochemistry*. 21:1909–1913.
11. Comper, W. D., and A. Veis. 1977. The mechanism of nucleation for *in vitro* collagen fibril formation. *Biopolymers*. 16:2113–2131.
12. Gelman, R. A., B. R. Williams, and K. A. Piez. 1979. Collagen fibril formation: Evidence for a multistep process. *J. Biol. Chem.* 254:180–186.
13. Eaton, W. A., and J. Hofrichter. 1978. Successes and failures of a simple nucleation theory of sickle cell hemoglobin gelation. *In* Biochemical and Clinical Aspects of Hemoglobin Abnormalities, W. S. Caughey, editor. Academic Press, Inc., New York. 443–457.
14. Ferrone, F. A., H. R. Sunshine, J. Hofrichter, and W. A. Eaton. 1980. Kinetic studies on photolysis-induced gelation of sickle cell hemoglobin suggest a new mechanism. *Biophys. J.* 32:361–380.
15. Abraham, F. F. 1974. Homogeneous Nucleation Theory. Academic Press, Inc., New York.
16. Zettlemoyer, A. C. 1969. Nucleation. Marcel Dekker, Inc., New York.
17. Morse, P. M., and H. Feshbach. 1953. Methods of Theoretical Physics. McGraw-Hill, Inc., New York. 2:999–1105.
18. Korn, E. D. 1982. Actin polymerization and its regulation by proteins from nonmuscle cells. *Physiol. Rev.* 62:672–737.
19. Tobacman, L. S., and E. D. Korn. 1983. The kinetics of actin nucleation and polymerization. *J. Biol. Chem.* 258:3207–3214.
20. Bevington, P. R. 1969. Data Reduction and Error Analysis for the Physical Sciences. McGraw-Hill, Inc., New York.
21. Miller, A. 1976. Molecular packing in collagen fibrils. *In* Biochemistry of Collagen. G. N. Ramachandran and A. H. Reddi, editors. Plenum Publishing Corp., New York. 85–136.
22. Wood, G. C. 1962. The heterogeneity of collagen solutions and its effect on fibril formation. *Biochem. J.* 84:429–435.
23. Comper, W. D., and A. Veis. 1977. Characterization of nuclei in *in vitro* collagen fibril formation. *Biopolymers*. 16:2133–2142.
24. Williams, B. R., R. A. Gelman, D. C. Poppke, and K. A. Piez. 1978. Collagen fibril formation: optimal *in vitro* conditions and preliminary kinetic results. *J. Biol. Chem.* 253:6578–6585.
25. Gelman, R. A., D. C. Poppke, and K. A. Piez. 1979. Collagen fibril formation *in vitro:* the role of the nonhelical terminal regions. *J. Biol. Chem.* 254:11741–11745.
26. Adachi, K., and T. Asakura. 1979. Nucleation-controlled aggregation of deoxyhemoglobin S: possible difference in the size of nuclei in different phosphate concentrations. *J. Biol. Chem.* 254:7765–7771.
27. Dykes, G., R. H. Crepeau, and S. J. Edelstein. 1978. Diameter of haemoglobin S fibres in sickled cells. *Nature (Lond.)*. 274:616–617.
28. Wellems, T. E., and R. Josephs. 1981. Polymorphic assemblies of double strands of sickle cell hemoglobin: manifold pathways of deoxyhemoglobin S crystallization. *J. Mol. Biol.* 153:1011–1026.
29. Ross, P. D., and A. P. Minton. 1977. Analysis of non-ideal behavior in concentrated hemoglobin solutions. *J. Mol. Biol.* 112:437–452.